4.3 Apparatus and Method

The final or 3rd generation version of our spectrometer was designed to take advantage of the electron timing techniques we have developed (see chapter 1 and appendix C) in addition to the cold local target. It is this combination that allows the true power of the momentum imaging technique to manifest itself. By combining the position and time measurements of the recoil ion and electron, we can determine the complete momentum vectors of *both* particles. Conservation of momentum requires that these quantities infer directly the momentum transfer vector of the projectile, the third body in the three-body collision. The experiment is therefore kinematically complete.

4.3.1 Setup

A scale rendering of the setup and a schematic diagram of the spectrometer is shown in figure 4.7. The super-bunched ion beam (along the z-axis) intersected a supersonic gas jet (y-axis) within the spectrometer as shown. Electrons and recoil ions originating from collisions between the projectiles and the target gas were then accelerated by the electric field produced by the spectrometer to the detectors. The conversion from position and TOF measurements to momentum was as described in previous chapters, except in the case of the non-linear electron TOF to P_x conversion which is described in appendix A.

The supersonic gas jet allowed us to have a localized target so that we knew the origin the collision event. In addition, the target was cold due to the expansion of the gas through a 30 μm nozzle, immediately followed by passage through a 0.5 mm skimmer directly below the spectrometer. Although not critical in the case of the molecule experiment, the low temperature of the gas was necessary in order to measure the soft electron production from helium targets. The momentum transfers in the helium case are quite small, and the resultant recoil ions can have energy changes much less than the energy of room-temperature thermal motion. The details of the target production are discussed in appendix B.

The spectrometer dimensions are shown in the figure. For the collision systems we measured, the momentum of both the recoil-ions and the electrons had the same order of magnitude, around 1 atomic unit. Because the recoil ion is 7,344 times more massive than the electron, its corresponding energy is less by the same factor. To account for this, we designed the spectrometer with a much longer recoil flight path than electron flight path. This allowed the recoils to spread out on the detector while at the same time enabling us to collect the electrons for the same field. The distance to the first grid of the electron detector from the target was 0.85 cm, while the distance to the recoil detector from the target was 80.4 cm, a factor of ~100 greater.

The voltages we applied to the spectrometer electrode are also labeled in the figure. The plates of the spectrometer were electrically connected in a chain via 250kΩ resistors. The final electrode (far right) in the chain was grounded. We

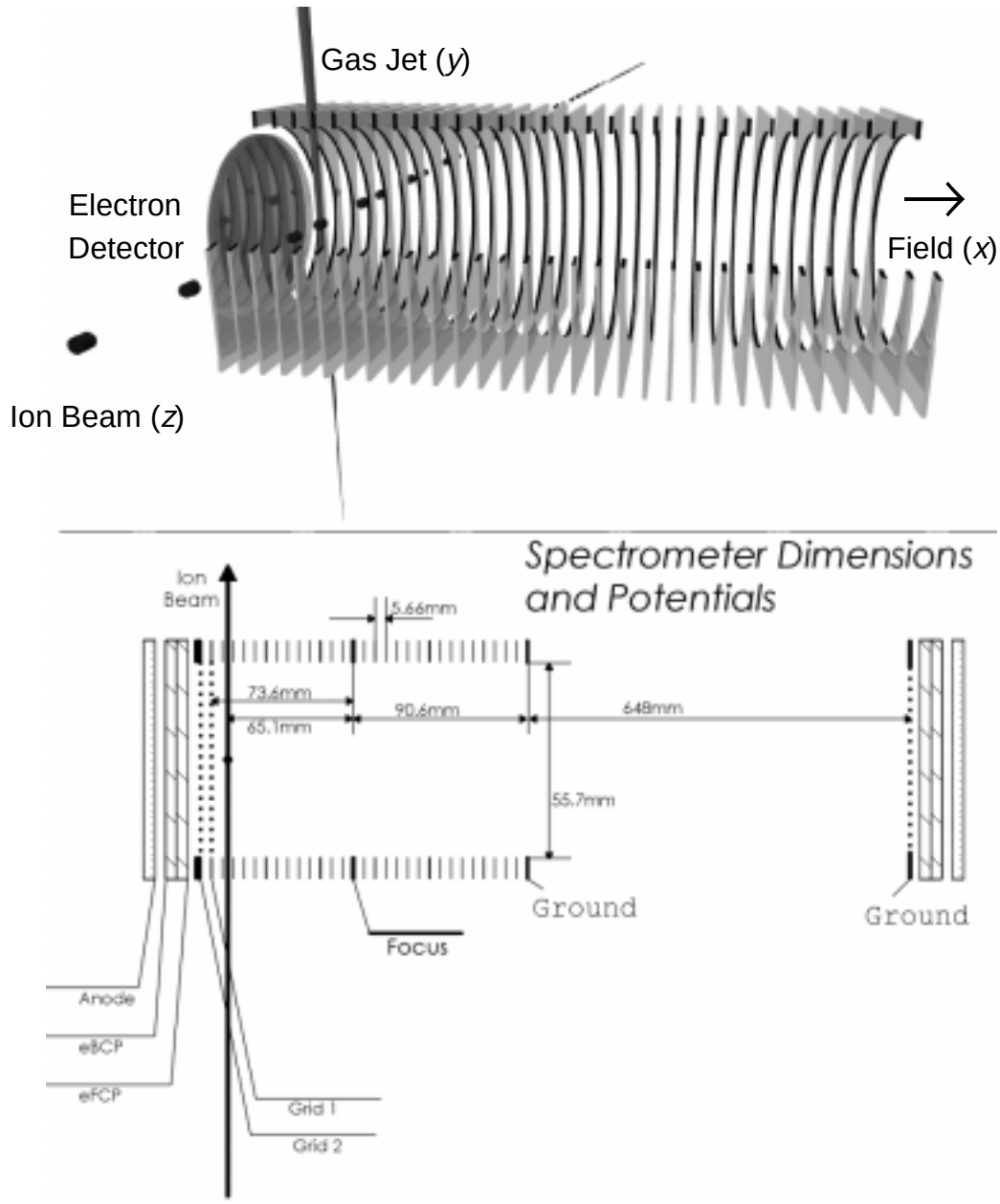

Figure 4.7: Scale rendering and schematic drawing of the 3rd generation spectrometer. Note the distance from the spectrometer to the recoil detector. The coordinate system we use is the same as in chapter 2: the x-axis is defined by the direction of the electric field, the y-axis is defined by the jet direction, and the z-axis is defined by the projectile ion beam. Due to the scale, the recoil detector is not shown in the upper figure.

applied voltage to the pusher (grid 1) and focus electrodes of the spectrometer, creating two uniform potential gradients on either side of the focus. Because there was no grid at the focus electrode to force a flat field, the change in electric field from one gradient to the next formed an electrostatic lens. This allowed us to spatially focus recoil ions (produced from different places in the 2 mm wide jet) onto the detector, while still maintaining separation of their momenta. The spectrometer was modeled with a *SIMION* simulation before it was built; these calculations are presented in appendix A.

Just as described in chapter 2, we measured the electron TOF relative to the master ion beam bunch clock. Again we used the LINAC to focus the projectile bunches in time. We measured the recoil ion flight time relative to the electron, and then subtracted the two times to get the true recoil ion flight time. Although the recoil ion flight time is much longer than that of the electron, this step was critical because the recoil ion distribution in time was then converted to transverse momentum along the field direction.

The conversions from position and time to momentum were essentially the same as described in chapter 2, except for the electron p_x. In this case, two grids were placed between the target and the first channel plate of the electron detector in order to have more control over the electron flight path. In retrospect, this only complicated the analysis. Electrons scattering between the grids produced echoes in the time spectrum. In addition, because the electron had to pass through three different field values, conversion of the flight time to momentum was nontrivial and was

accomplished via a simulation. The same simulation served to calculate the edge of the electron detector in momentum space, allowing for another check on our results. We used a capture reaction to calibrate the position to momentum conversion for the recoil ions. These and other calibrations are presented in appendix A.

The experimental parameters for each of the data runs used for the final results are presented in the table below. They are taken directly from the data book.

Run #	282	293	302
Beam	1 MeV H^+	5 MeV H^+	19 MeV F^{9+}
V_{RCP}	1900/ 20/ 0	1900 /20 / 0	1900 /20 / 0
V_{eCP}	2650/ 2600/ 700	2650/ 2600/ 700	2650/ 2600/ 700
Grid 1	500	500 V	1000 V
Grid 2	541	498 V	995 V
Focus	372	372 V	744 V
e^- Rate	5 kHz	3 kHz	8 kHz
R Rate	1 kHz	1.5 kHz	2 kHz
TAC Rate	10 Hz	50 Hz	80 Hz
eR TAC Range	200 nsec	200 nsec	200 nsec
eP TAC Range	100 nsec	100 nsec	100 nsec
Beam Current	2 pA	40 pA	< 1 pA

Note that the pusher voltage required for the fluorine system was larger than for that of the protons. The electrons in this case had a substantially larger forward momentum, and the higher field was required to get the majority of the distribution on the detector. Further details on the measurements may be found in the appendices.